

Lawrence Berkeley National Laboratory

Recent Work

Title

Crystallography of Co/Pt Multilayers and Nanostructures

Permalink

<https://escholarship.org/uc/item/0q3954r8>

Authors

Zhang, B.

Krishnan, K.M.

Farrow, R.F.C.

Publication Date

1992-04-01



Lawrence Berkeley Laboratory

UNIVERSITY OF CALIFORNIA

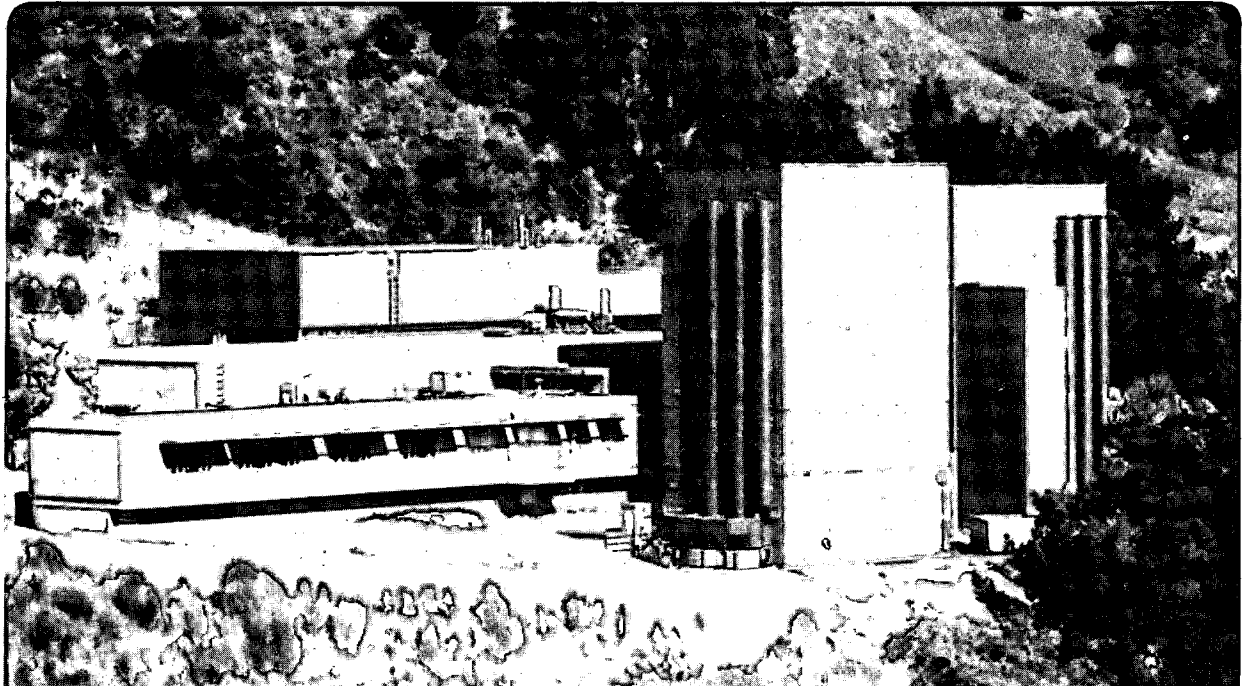
Materials Sciences Division National Center for Electron Microscopy

Presented at the Frontiers of Electron Microscopy in
Materials Science, Berkeley, CA, April 21-24, 1992,
and to be published in the Proceedings

Crystallography of Co/Pt Multilayers and Nanostructures

B. Zhang, K.M. Krishnan, and R.F.C. Farrow

April 1992



Prepared for the U.S. Department of Energy under Contract Number DE-AC03-76SF00098

REFERENCE COPY 1
Does Not 1
Circulate 1
Bldg. 50 Library.
LBL-32290
Copy 1

DISCLAIMER

This document was prepared as an account of work sponsored by the United States Government. Neither the United States Government nor any agency thereof, nor The Regents of the University of California, nor any of their employees, makes any warranty, express or implied, or assumes any legal liability or responsibility for the accuracy, completeness, or usefulness of any information, apparatus, product, or process disclosed, or represents that its use would not infringe privately owned rights. Reference herein to any specific commercial product, process, or service by its trade name, trademark, manufacturer, or otherwise, does not necessarily constitute or imply its endorsement, recommendation, or favoring by the United States Government or any agency thereof, or The Regents of the University of California. The views and opinions of authors expressed herein do not necessarily state or reflect those of the United States Government or any agency thereof or The Regents of the University of California and shall not be used for advertising or product endorsement purposes.

Lawrence Berkeley Laboratory is an equal opportunity employer.

DISCLAIMER

This document was prepared as an account of work sponsored by the United States Government. While this document is believed to contain correct information, neither the United States Government nor any agency thereof, nor the Regents of the University of California, nor any of their employees, makes any warranty, express or implied, or assumes any legal responsibility for the accuracy, completeness, or usefulness of any information, apparatus, product, or process disclosed, or represents that its use would not infringe privately owned rights. Reference herein to any specific commercial product, process, or service by its trade name, trademark, manufacturer, or otherwise, does not necessarily constitute or imply its endorsement, recommendation, or favoring by the United States Government or any agency thereof, or the Regents of the University of California. The views and opinions of authors expressed herein do not necessarily state or reflect those of the United States Government or any agency thereof or the Regents of the University of California.

Crystallography of Co/Pt Multilayers and Nanostructures

Bing Zhang, K.M. Krishnan, and R.F.C. Farrow*

Materials Science Division
National Center for Electron Microscopy
Lawrence Berkeley Laboratory
University of California, Berkeley, CA 94720

*IBM Almaden Research Center
650 Harry Road
San Jose, CA 95120

Submitted for *Frontiers in Electron Microscopy*
Berkeley, CA
4/21-4/24/92

This work was supported in part by the Director, Office of Energy Research, Office of Basic Energy Sciences, Materials Science Division of the U.S. Department of Energy under Contract No. DE-AC03-76SF00098.

CRYSTALLOGRAPHY OF Co/Pt MULTILAYERS AND NANOSTRUCTURES

Bing Zhang, Kannan M. Krishnan and Robin F. C. Farrow*

Materials Sciences Division, National Center for Electron Microscopy, Lawrence Berkeley
Laboratory, Berkeley, CA 94720

* IBM Almaden Research Center, 650 Harry Road, San Jose, CA 95120

Abstract

Atomically engineered nanostructures and multilayers of Co/Pt exhibit strong perpendicular anisotropy. This unique property, that determines their potential as a magneto-optic recording media, is dependent on a variety of microstructural parameters that include the overall crystallography, thickness of the layers, orientation, defect formation, interface reactions etc. A series of Co/Pt multilayer samples with different thickness of the Co layer were studied by electron diffraction. It has been determined that the Co layers persists in the fcc structure up to a thickness of 50 Å. As the thickness is varied from 3Å to 50Å in the multilayers, the Co film gradually relaxed to its bulk lattice parameter. (111) twinning and lattice strain at the interfaces between Pt and Co layers are also observed. The symmetry forbidden reflections observed at $1/3\{224\}$ positions in [111] zone diffraction patterns of the multilayer are due to (111) twinning and compositional modulations along the multilayer growth direction.

Introduction

Ultrathin multilayers of Co and Pt are good candidate materials for magneto-optic recording. These films exhibit anisotropy of magnetization perpendicular to the film plane and a square hysteresis loop. The origin of these desirable properties is not well understood but it is believed that they are mainly influenced by microstructural and crystallographic parameters of the multilayer stack [1]. These include the thickness of the individual layers, interface structure,

chemistry, strain, and texture of the film, etc. The correlations of structure, morphology, and growth-mode of such films with good properties present an on-going challenge to materials researchers working with ultrathin magnetic film structures. Films with a few Ångstroms of cobalt alternatively layered with several Ångstroms of Pt exhibit perpendicular anisotropy; thicker films do not. In order to make better films for future MO recording, an improvement of the interface-induced anisotropy and a better understanding of the attendant mechanisms are required.

In this paper we focus on the crystallography of a series of $(\text{Co}_x\text{Pt}_y)_n$ multilayers, where x, y represent the thickness of individual Co and Pt layers in Ångstroms and $n=15$ is the number of repeats. Five different samples with $x=3, 6, 9, 12$, and $y=16-18$, as well as $(\text{Co}_{50}/\text{Pt}_{50})_4$ were studied. These samples exhibit a monotonic decrease in perpendicular anisotropy with increase in Co layer thickness. Both plan view and cross-section samples were studied. The variation in the crystallographic structure of the multilayers obtained by conventional electron diffraction method will be used to understand this range in magnetic properties. Characterization of the detailed interface structure, interface magnetic coupling as well as the attendant mechanisms of perpendicular anisotropy will be the next step in this research.

Experimental

All $(\text{Co}_x\text{Pt}_y)_n$ multilayer samples were grown by molecular beam epitaxy on GaAs $(\bar{1}\bar{1}\bar{1})$ substrate with a ~ 200 Å thick Ag buffer layer. Plan-view and cross-section TEM samples were prepared by mechanical thinning and ion-milling. All electron diffraction experiments were performed on a JEOL 200CX TEM and the computer simulation of the diffraction patterns was obtained by using MacTempas and Crystalkit software packages [2].

Results and discussion

All five samples have a grain size of 200-300Å, but the plan-view SAD patterns averaged over many grains show a single crystal diffraction pattern and this is indicative of very good

epitaxy during the growth processes. The plan-view [111] zone axis SAD patterns taken from the whole series of Co_xPt_y samples are shown in Fig. 1 (a-e).

For $x=3$ and $y=18$, a single crystal SAD pattern (Fig. 1a) corresponding to the face-centered cubic platinum structure is observed. The Co monolayer is accommodated in the Pt lattice and is not separately resolved in the diffraction pattern. However, due to the 10% lattice parameter difference between Co_{fcc} and Pt_{fcc} this accommodation could give rise to a large amount of strain at the interface. In principle, the resulting strain field will exhibit a periodicity identical to the compositional variation along the film growth direction. The diffraction pattern from the $\text{Co}_6\text{Pt}_{18}$ thin film (Fig. 1b) indicates the beginning of the relaxation of the Co layer. The {220} diffraction spots in Figs.1b are elongated along the $\langle 220 \rangle$ directions. For $x=6$, with approximately 3 MLs of Co stacked along the [111] growth direction, Co begins to relax to its own Co_{fcc} lattice parameter while being coherent and retaining the same f.c.c. structure as the Pt layer. This is a transition state before the formation of an independent thin Co crystal. When the thickness of Co reaches, more or less, 4 MLs stacked along [111] in the sample $\text{Co}_9\text{Pt}_{16}$, as shown in Fig.1c, the interior of the Co layer has already developed its own lattice. This gives rise to the distinct {220} type intensities. Two sets of intensity maxima in Fig.1c representing d_{220} reflections of Pt_{fcc} and Co_{fcc} , are clear in the diffraction pattern. However, the spacing corresponding to the {220} lattice planes within the Co layer is intermediate between d_{220} of Pt and d_{220} of Co. Figs 1 (d-e) are the [111] zone diffraction patterns taken from the samples of $\text{Co}_{12}\text{Pt}_{18}$, and $\text{Co}_{50}\text{Pt}_{50}$. With increasing Co layer thickness, the two diffraction spots from Pt and Co are more distinct and the intensity distribution between the two are more even. The separation between the {220} spots of Co and Pt increases slightly from Figs.1(c-d) to Fig.1e. The $\{220\}_{\text{Co}}$ positions in (e) corresponds to the equilibrium lattice parameter in bulk Co. The diffuse intensity between $\{220\}_{\text{Pt}}$ and $\{220\}_{\text{Co}}$ diffraction spots in Figs. 1(b-e) arises mainly from the interface lattice strain. One common feature in Figs. 1(a-e) is that, in spite of the thickness changes of the Co layers, all diffraction patterns

exhibit fairly strong intensity at $1/3\{224\}$ positions. This will be discussed in a later part of this paper.

It can be argued that a more realistic evaluation of the crystallography of the film can be obtained by studying the films "as is" with the GaAs and Ag buffer layer in place. Figs. 2(a-d) show the [111] SAD patterns in the same sequence as in Fig.1, but with overlapping substrate and magnetic film. In addition to the diffraction from the multilayer, spots from the Ag buffer layer and GaAs substrate are very clear. The SAD patterns are more complicated due to double diffraction from the different components of the multilayer stack. For instance, both incident and diffracted beams coming out of the first layer of the sample (such as Co_xPt_y), which has a different lattice spacing from the second (such as the Ag buffer) and the third (such as the substrate) will serve as incident beams for the subsequent layers. If a diffracted (220) beam from the film is scattered again by the same type of (220) lattice planes of the buffer layer - which has a different value of lattice spacing from that of the film, the second diffracted beam will not contribute intensity back to the transmitted beam but rather give rise to an additional spot in the diffraction pattern corresponding to the difference of the lattice spacings between the film and the buffer layer. This explains the set of spots immediately around the transmitted beam. By similar double diffraction considerations, all extra spots in the patterns in Fig. 2 can be indexed and understood. However, in these series of measurements (Figs. 2 a-d), the observations made earlier (Figs. 1a-d) remain unchanged: the gradual relaxation of the Co layer from being accommodated by Pt_{fcc} lattice to its own distinct Co_{fcc} lattice is maintained and the streaking due to the strain in the vicinity of the interfaces is also observed. The effect of the removal of the substrate and the Ag buffer layer is marginal and the accommodation at the interface seems to dominate the plan view diffraction patterns.

Twinning was observed in similar multilayer films and it was pointed out [3] that during the growth, (111)-twin related islands nucleate in the Ag layer and propagate through the multilayer sequence. Overall, two different types of grains rotated by 180° degrees about the [111] axis of

one grain with respect to the other are generated and this results in a polycrystalline microstructure in the image and a single crystal diffraction pattern. In addition to twinning, the 180° relationship between the grains or the 6-fold symmetry of the film is made possible by "double positioning" in the stacking along the [111] axis [4,5]. This has been confirmed by *in situ* RHEED and LEED measurements [2,6]. The cross-section diffraction patterns from $(\text{Co}_{50}/\text{Pt}_{50})_4$, in Fig. 4, clearly show the same type of (111) twins in Ag, Pt and Co. Hence, it is concluded that, during the growth process, four different stacking sequences are possible: 1) ABCABCABC..., 2) ACBACBACB..., 3) BCABCABCA..., 4) BACBACBAC..

As mentioned earlier, one common feature in Figs.1(a-e) is that regardless of the thickness of the Co layers, all plan-view diffraction patterns exhibit extra spots at $1/3\{224\}$ positions. These additional reflections were observed earlier [6,7] and attributed to surface steps and/or stacking faults. We believe that the intensities of the extra reflections are too strong to be explained as simple surface steps and/or stacking faults. An alternative view [4] is that these extra spots are generated by double diffraction i.e., the (111) electron beam is double diffracted by the allowed $1/3(\bar{1}\bar{5}1)$ twin reflection, thus $(111)+1/3(\bar{1}\bar{5}1) = 1/3(2\bar{2}4)$.

Computer simulations of the diffraction patterns, using the well established multislice method, including the limited dynamical interactions between the transmitted and diffracted beams, were carried out in an attempt to account for the effect of twinning and compositional periodicity. Fig. 3a is a simulated diffraction pattern for 87 Pt monolayers stacked in a typical ABCABC sequence along the [111] direction. A typical [111] zone axis pattern is observed. We then arranged the 87 Pt MLs in such a way that a (111) twin plane was located halfway through the stack. The result of this simulation (Fig. 3b), clearly shows additional intensities at $1/3\{224\}$ positions with an overall 3-fold symmetry. In addition, inserting a monolayer of Co after every six Pt layers to simulate the $\text{Co}_3\text{Pt}_{18}$ multilayer resulted (Fig. 3c), in six extra spots at $1/3\{224\}$ positions. Based on these results we conclude that the extra diffraction spots are mainly due to

(111) twinning, composition modulation along [111] and dynamical interactions of electron beams within the multilayer.

These extra reflections disappeared when the substrate and the film overlap, as shown in Fig. 2 (a-d). The extra intensities originate from the thin multilayer ($\sim 300\text{\AA}$) only and when the overlap occurs, this effect is comparatively weak and it is very likely overwhelmed by strong scattering from the large volume of untwinned GaAs and the strong dynamical interactions of the scattered beams from the various components of the stack. Therefore the intensity of those reflections is very low compared to the regular diffraction maxima in Fig. 2 (a-d).

One unresolved question is the polymorphic form of Co in the multilayers. F.J. Lamelas et. al, [8] in their study of Co/Cu thin films, pointed out that Co in the multilayers keeps a metastable fcc stacking up to a thickness of 20\AA , above which, it will revert to the more stable hcp stacking along the normal of the film.

Cross-section samples of $(\text{Co}_{50}/\text{Pt}_{50})_4$ were examined to determine the crystal structure of Co in the multilayer. Fig. 4a is a typical $[1\bar{1}0]$ SAD. There are 4 sets of reflections in the pattern - the strong single crystal $[110]$ zone axis diffraction spots are from GaAs and the other three sets of (111) twinned diffraction patterns are from Ag, Pt and Co respectively. The diffraction spots from Co compared to those from Pt are more diffuse and more elongated along $[111]$ in spite of the shape effect being equal for identical thickness of Co and Pt. This indicates that there is greater lattice distortion or strain in the Co layer than in the Pt layer. Fig. 4b is a $[111]$ SAD pattern from the cross-section sample similar to those in Fig 2 (a-d). However, much less dynamical interactions is expected because the electron beam is incident only about 20 degrees off the interface plane. In Fig. 4a the incident beam is exactly parallel to the interface in the multilayer and in this configuration, there is a minimum chance for the incident and diffracted beams to go through different layers of the film. However, a few double diffraction spots around the transmission beam in Fig. 4b due to the small tilting of the cross-section sample are observed. This argument can also be applied to the $[2\bar{3}\bar{3}]$ SAD shown in Fig. 4c. All cross-section

diffraction patterns show strong evidence that Co in the multilayer exhibit the same crystal structure as Pt and Ag including the (111) twinning. It can be concluded that Co_{fcc} structure persists upto a thickness of 50 Å contrary to what had been suggested earlier [8].

Conclusions

Electron diffraction studies of plan view and cross-section samples of ultrathin $(\text{Co}_x\text{Pt}_y)_n$ multilayers provide important new insight into their crystallographic structure. They include

1) Starting from being virtually indistinguishable from Pt_{fcc} ($x=3\text{Å}$), the interior of the Co layer gradually relaxes ($x=6,9, 12,50$) to a lattice parameter corresponding to bulk Co_{fcc} . Interface strain between Co and Pt is fairly strong and gives rise to diffuse intensity between the {220} Pt and Co spots for the entire range of Co layer thicknesses.

2) (111) twinning is an integral part of the growth for all components of the multilayer stack (Co, Pt, Ag) and combined with 'double positioning' gives rise to 4 different stacking sequences.

3) Dynamical interactions within the multilayers are strong. When combined with twinning and chemical variation along the [111] direction the extra reflection at $1/3\{224\}$ positions can be explained.

4) Cross-section diffraction patterns give important information about the structure and defects within the multilayer. Co maintains the fcc crystal structure at least up to a thickness of 50Å rather than transform to the more stable hcp form.

Acknowledgements

This research was supported by the Director Office of Energy Research, Office of Basic Energy Sciences, Materials Sciences Division of the US Department of Energy under contract No. DE-AC03-76SF00098.

References

- [1] C. J. Lin, G. L. Gorman, C. H. Lee, R. F. C. Farrow, E. E. Marinero, H. V. Do, and H. Notarys, and C. J. Chien, *J. of Magnetism and magnetic materials*, Vol. 193 (1991) P. 194.
- [2] Available from Total Resolution, 20 Florida Ave, Berkeley, CA 94707.
- [3] N. H. Cho, K. M. Krishnan, C. H. Lee and R. F. C. Farrow, *Appl. Phys. Lett.*, Vol. 60 (1992)
- [4] D. W. Pashley and M. J. Stowell, *Phil. Mag.*, Vol. 8 (1964) p. 1605.
- [5] I. V. Sabinins, A. K. Gutakovskii, Yu. G. Sidorovm, and V. D. Kuzmin, *Phys. Stat. Sol. (a)* Vol.126, (1991), p. 181.
- [6] C. H. Lee, R. F. Farrow, C. J. Lin, E. E. Marinero, and C. J. Chien, *Physical Review B*, Vol. 42, No. 17 (1990) p. 11384.
- [7] C. J. Chien, R. F. C. Farrow, C. H. Lee, C. J. Lin and E.E. Marinero, *J. of Magnetism and Magnetic Materials* Vol. 93 (1991) p. 47
- [8] F. J. Lamelas, C. H. Lee, Hui He, W. Vavra, and Roy Clarke, *Phy. Rev. B*, Vol. 40, No. 8, (1989) P. 5837.

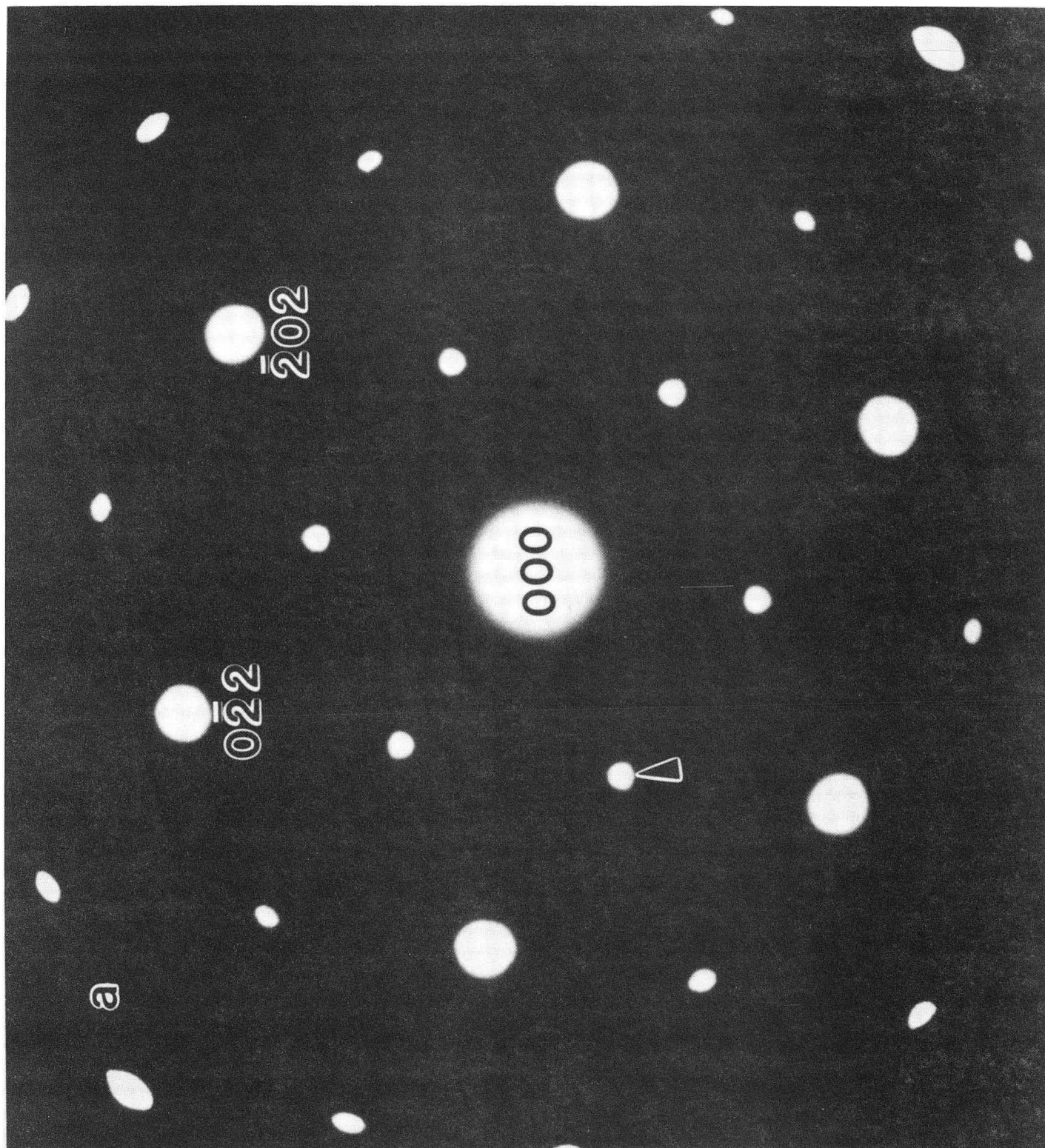
Figure Captions

Fig.1 [111] zone diffraction patterns from the multilayer of, a) $(\text{Co}_3\text{Pt}_{18})_{15}$ sample; b) $(\text{Co}_6\text{Pt}_{16})_{15}$ sample, the $\{220\}$ reflections elongated along $\langle 220 \rangle$ directions; c) $(\text{Co}_9\text{Pt}_{16})_{15}$, weak and distinct intensities representing $\{220\}$ reflections from Co in addition to Pt; d) $(\text{Co}_{12}\text{Pt}_{16})_{15}$ sample, showing a further separation between the two sets $\{220\}$ diffraction spots from Pt and Co, as well as the diffuse intensities between $\{220\}_{\text{Pt}}$ and $\{220\}_{\text{Co}}$; e) $(\text{Co}_{50}\text{Pt}_{50})_4$ sample, the strong $\{220\}$ reflections from Co corresponding the equilibrium lattice parameter in bulk Co_{fcc} . The extra reflections at $1/3\{224\}$ positions are due to (111) twinning and the composition variation along the normal of the multilayer.

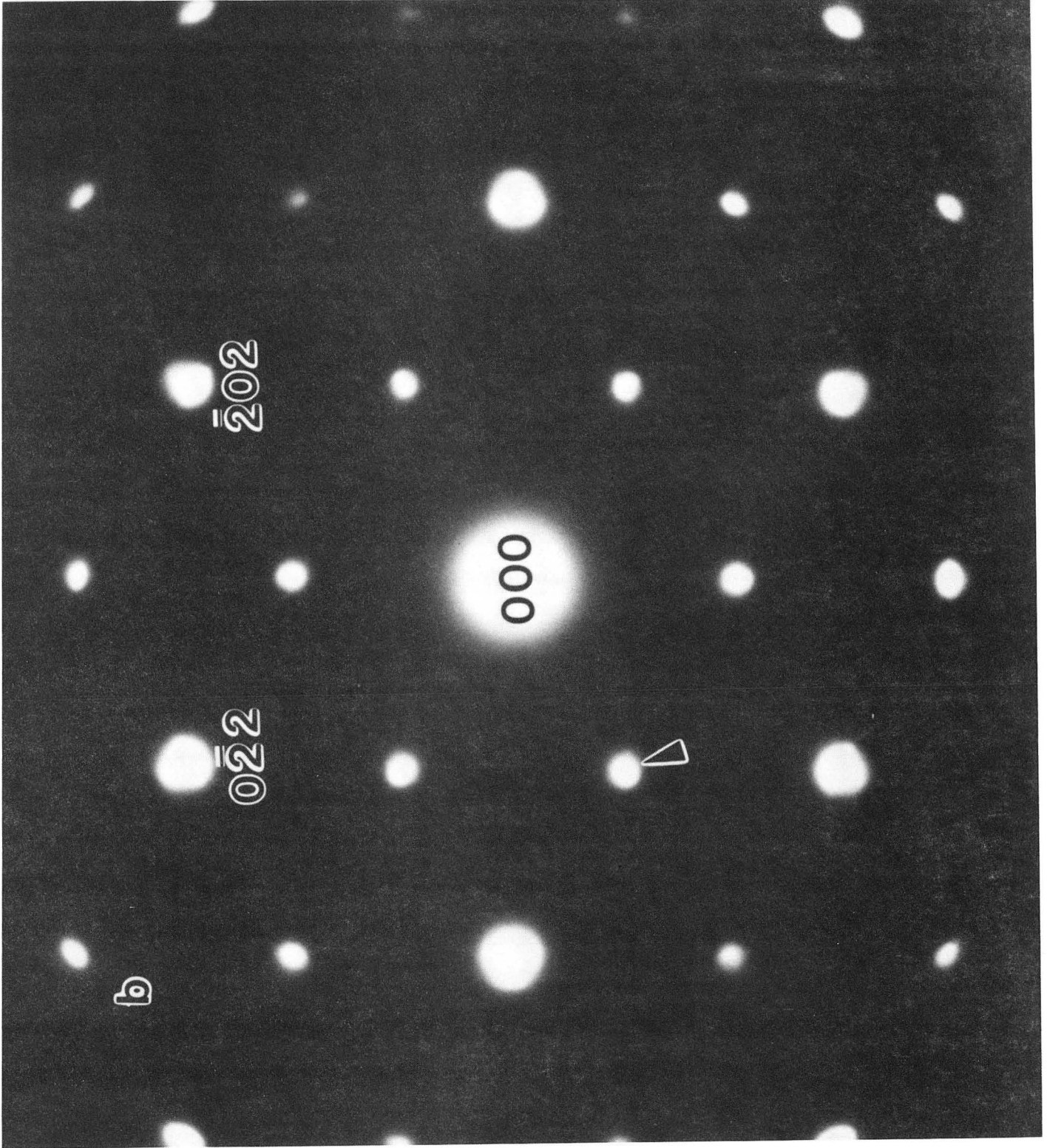
Fig. 2 [111] zone diffraction patterns from the overlapped multilayer, Ag buffer and GaAs substrate, a) $(\text{Co}_3\text{Pt}_{18})_{15}$; b) $(\text{Co}_9\text{Pt}_{16})_{15}$; c) $(\text{Co}_{12}\text{Pt}_{16})_{15}$; d) $(\text{Co}_{50}\text{Pt}_{50})_4$, showing many double diffraction spots as a result of strong dynamical interaction among electron beams.

Fig. 3 Computer simulation of [111] zone diffraction patterns; a) normal ABCABC... stacking of 87 monolayers of pure Pt along [111] direction; b) normal stacking as in a) but with a (111) twin plane in the middle of the 87 slices of pure Pt; c) stacking 6 monolayers of Pt and 1 monolayer of Co to simulate the configuration $(\text{Co}_3\text{Pt}_{18})_{15}$ and introducing a (111) twin plane in the middle of the 87 slice sequence.

Fig. 4 Cross- section diffraction patterns from $(\text{Co}_{50}\text{Pt}_{50})_4$ indicating that Co has a fcc structure; a) $(1\bar{1}0)$ zone, showing 4 sets of diffraction spots and the ones that correspond to Ag, Pt, Co, are twinned; b) (111) zone, similar to those in Fig.2, but with reduced double diffraction effect. C) $(22\bar{3})$ zone axis pattern.



a



b

Figure 1b

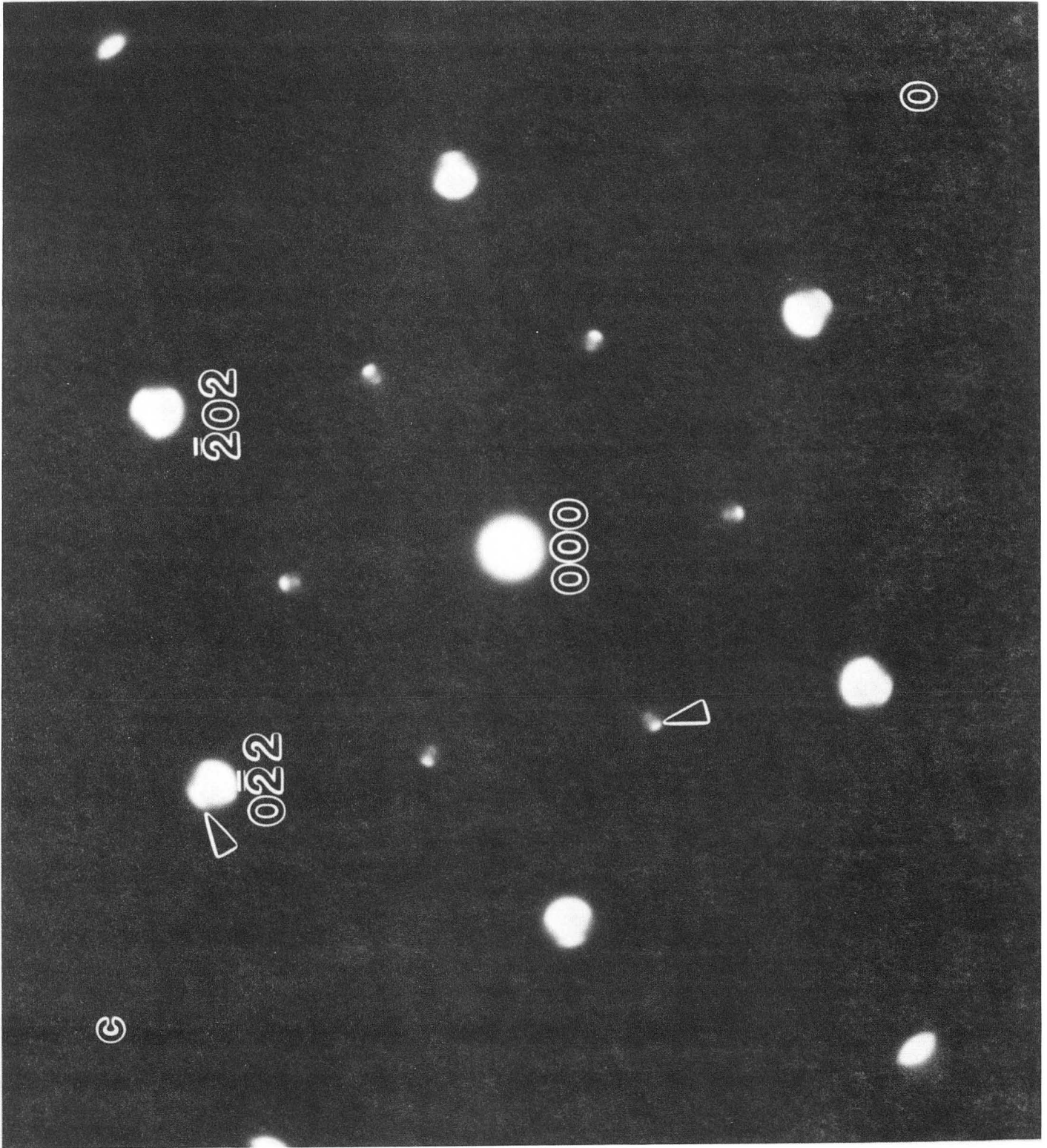
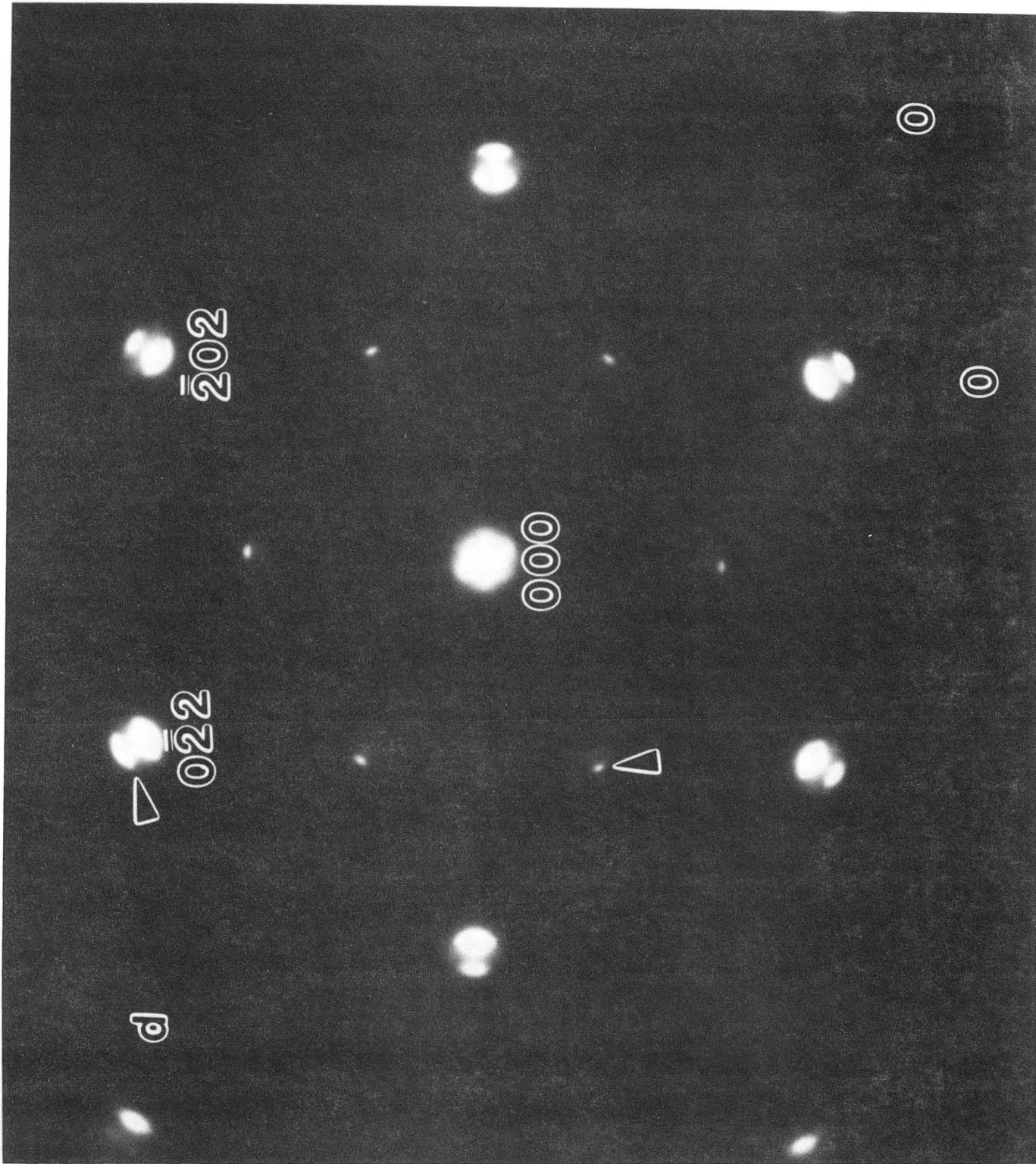


Figure 1c



XBB 925-3831

Figure 1d

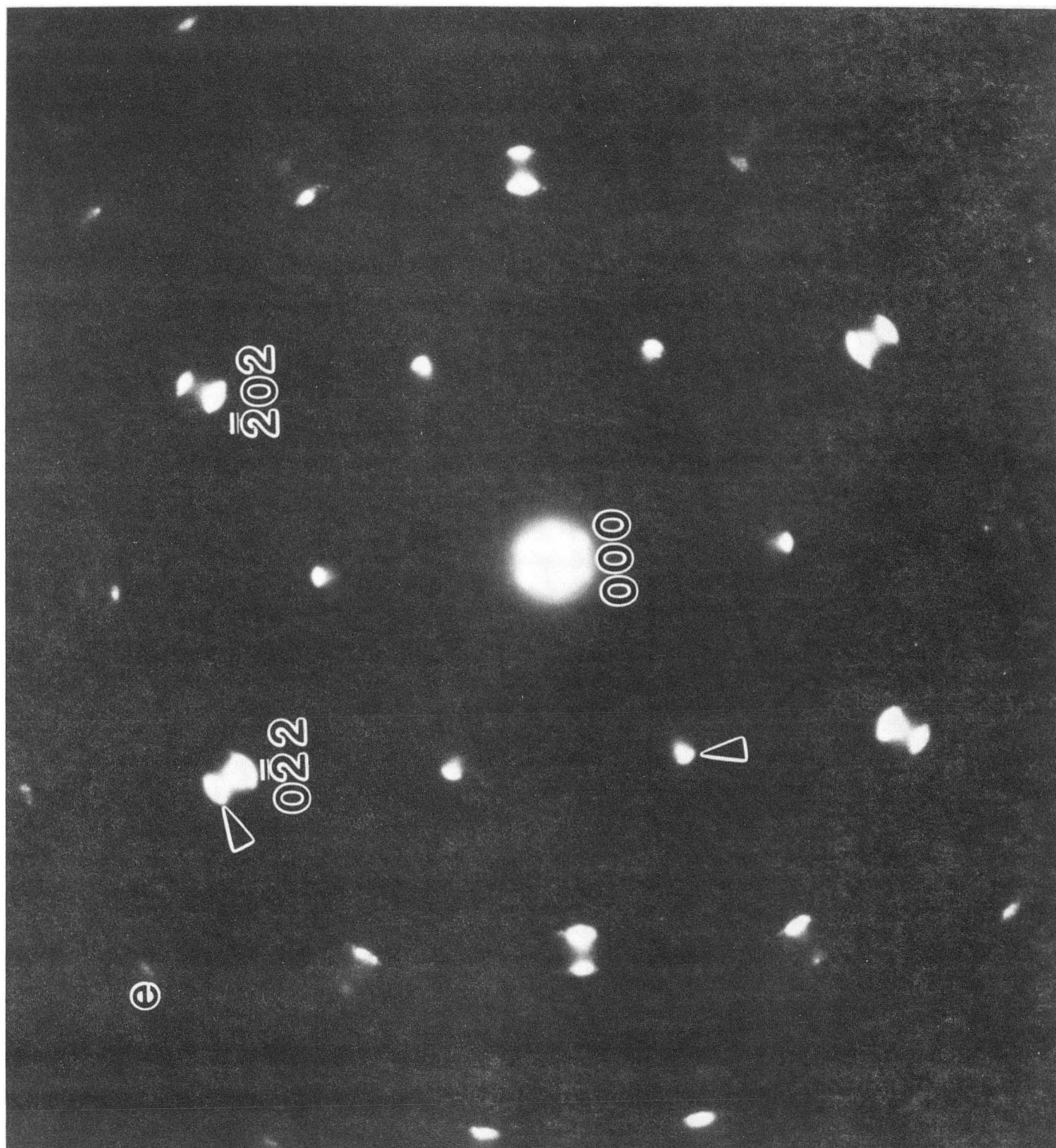
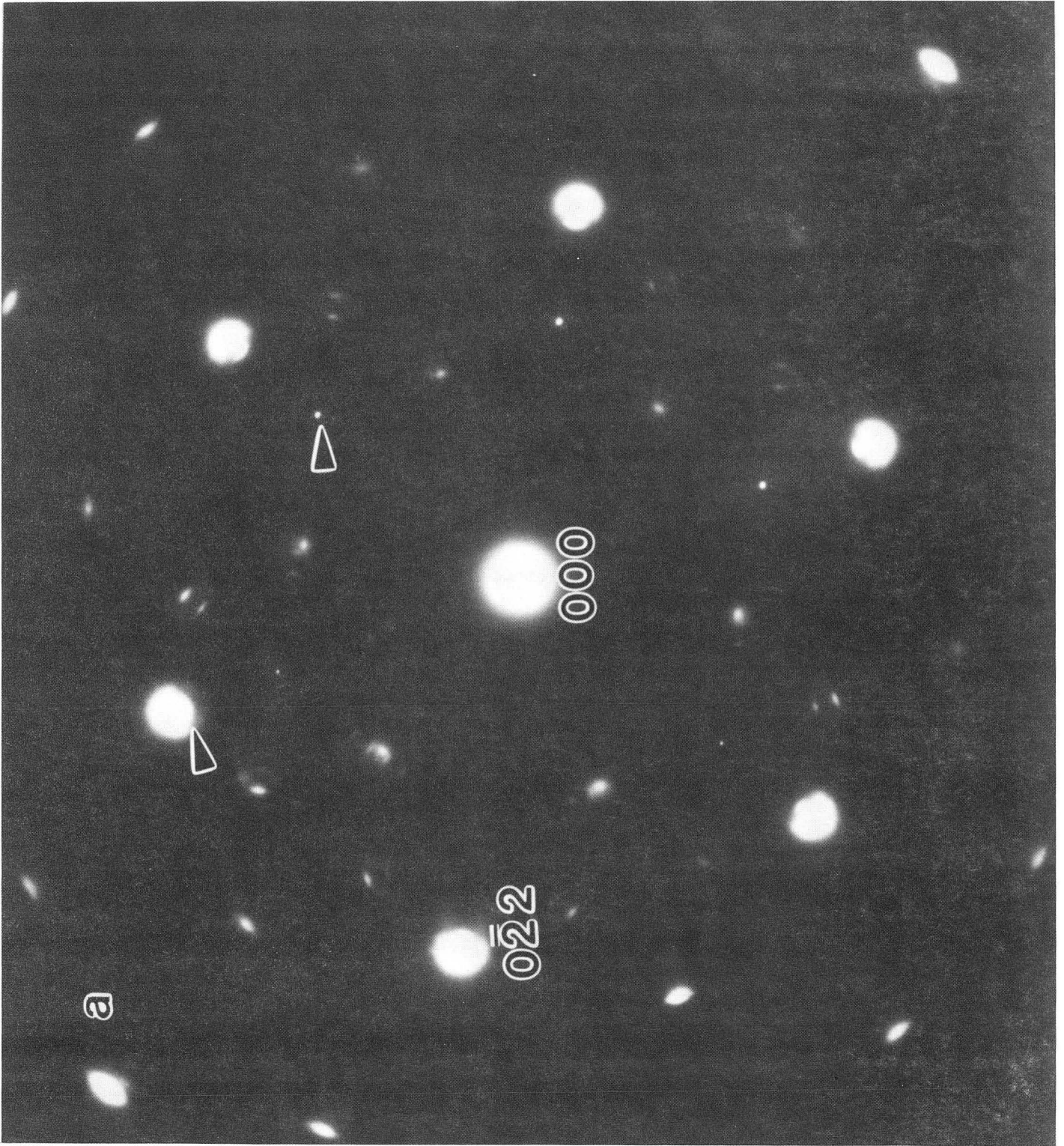


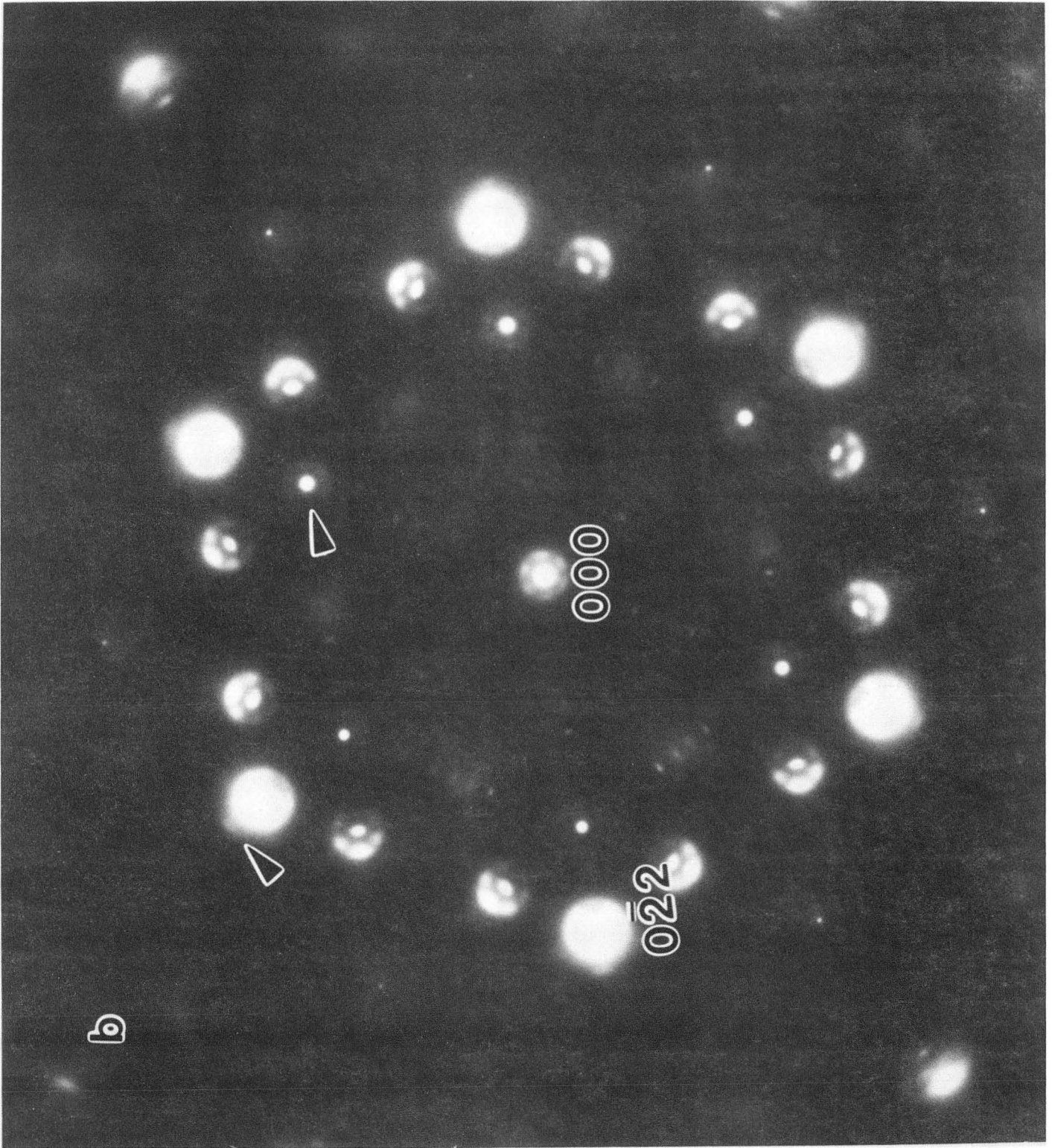
Figure 1e

XBB 925-3832



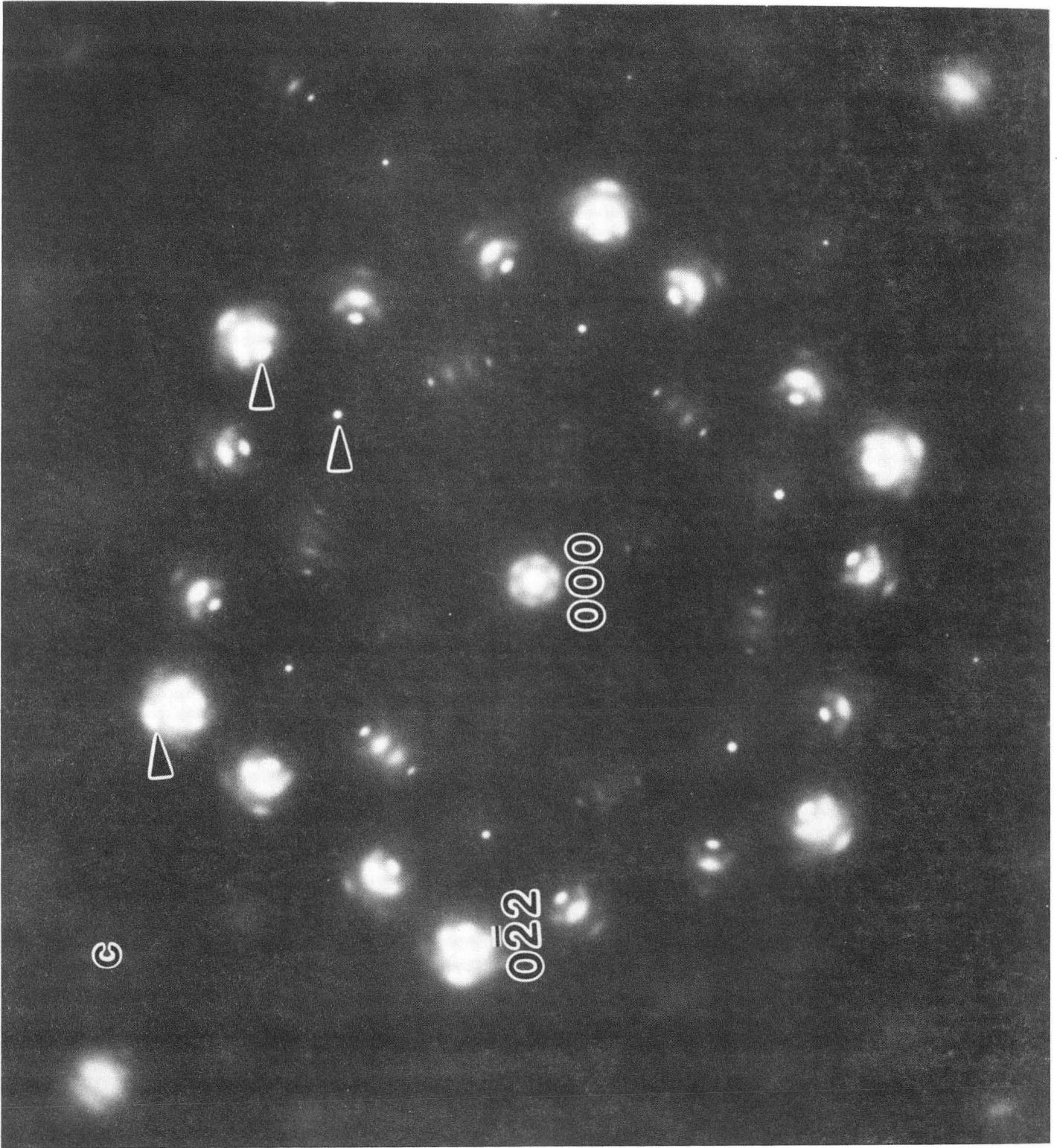
XBB 925-3833

Figure 2a



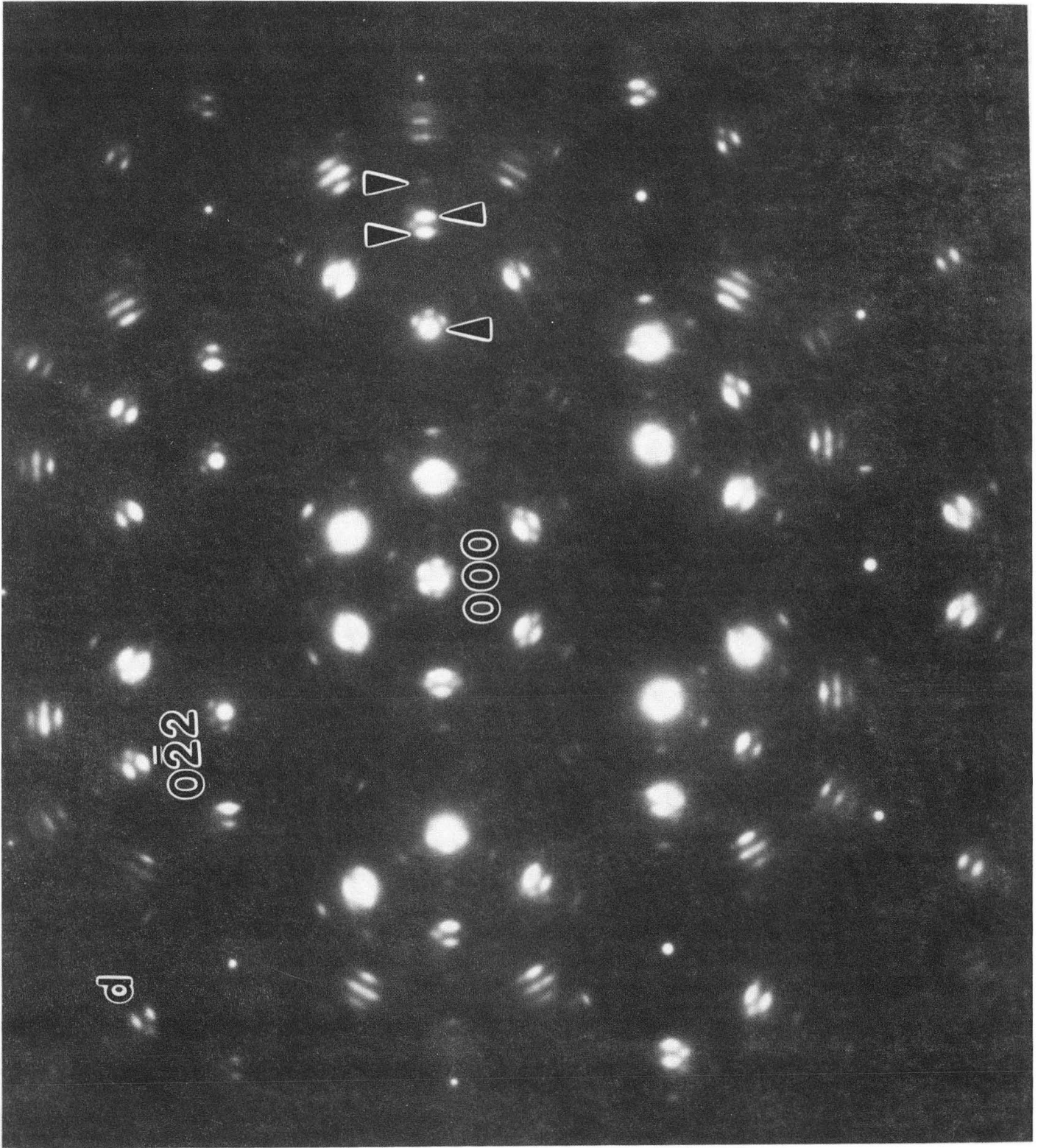
XBB 925-3834

Figure 2b



XBB 925-3835

Figure 2c



XBB 925-3836

Figure 2d

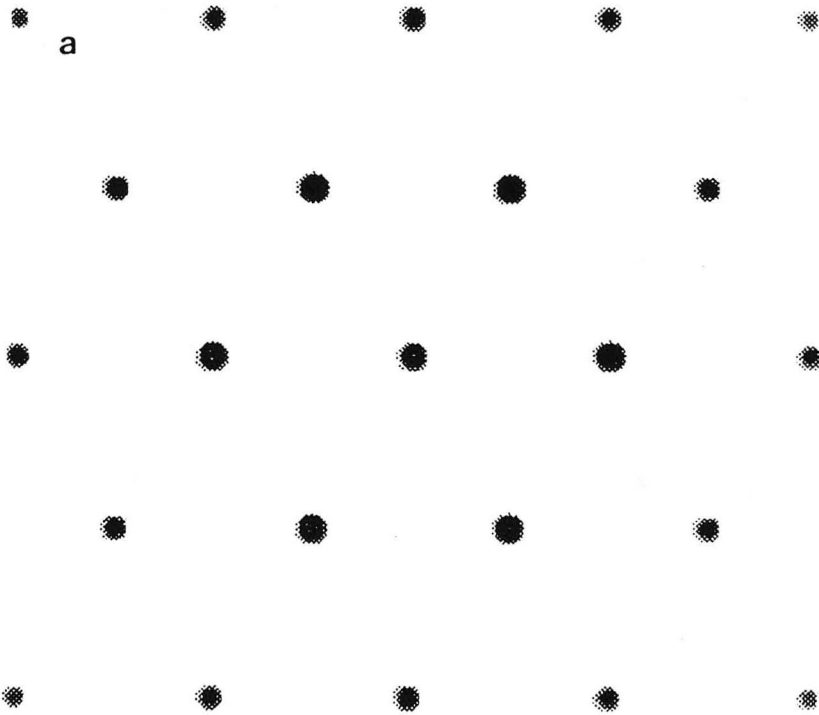


Figure 3a

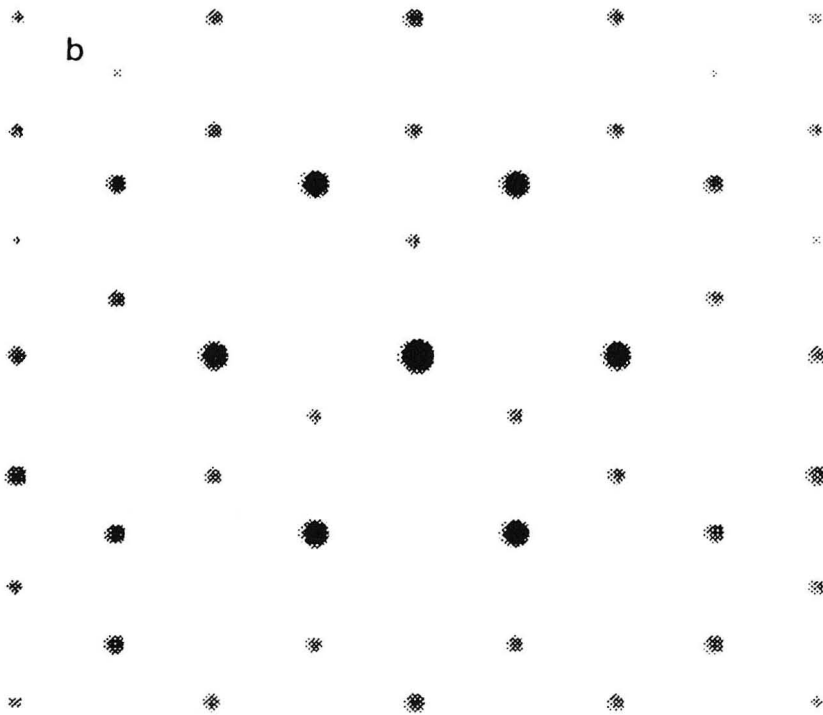


Figure 3b

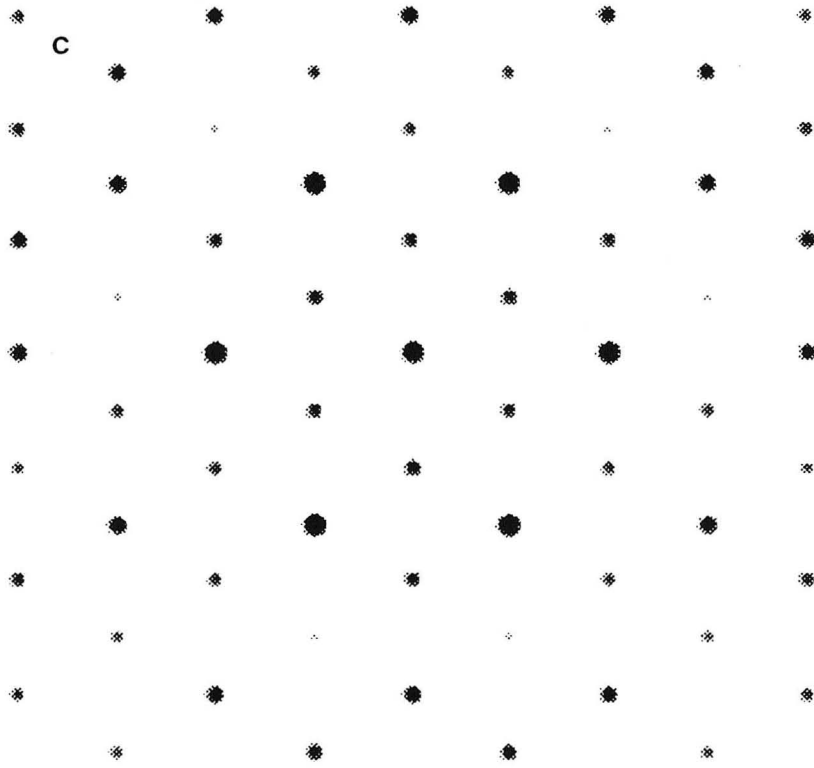
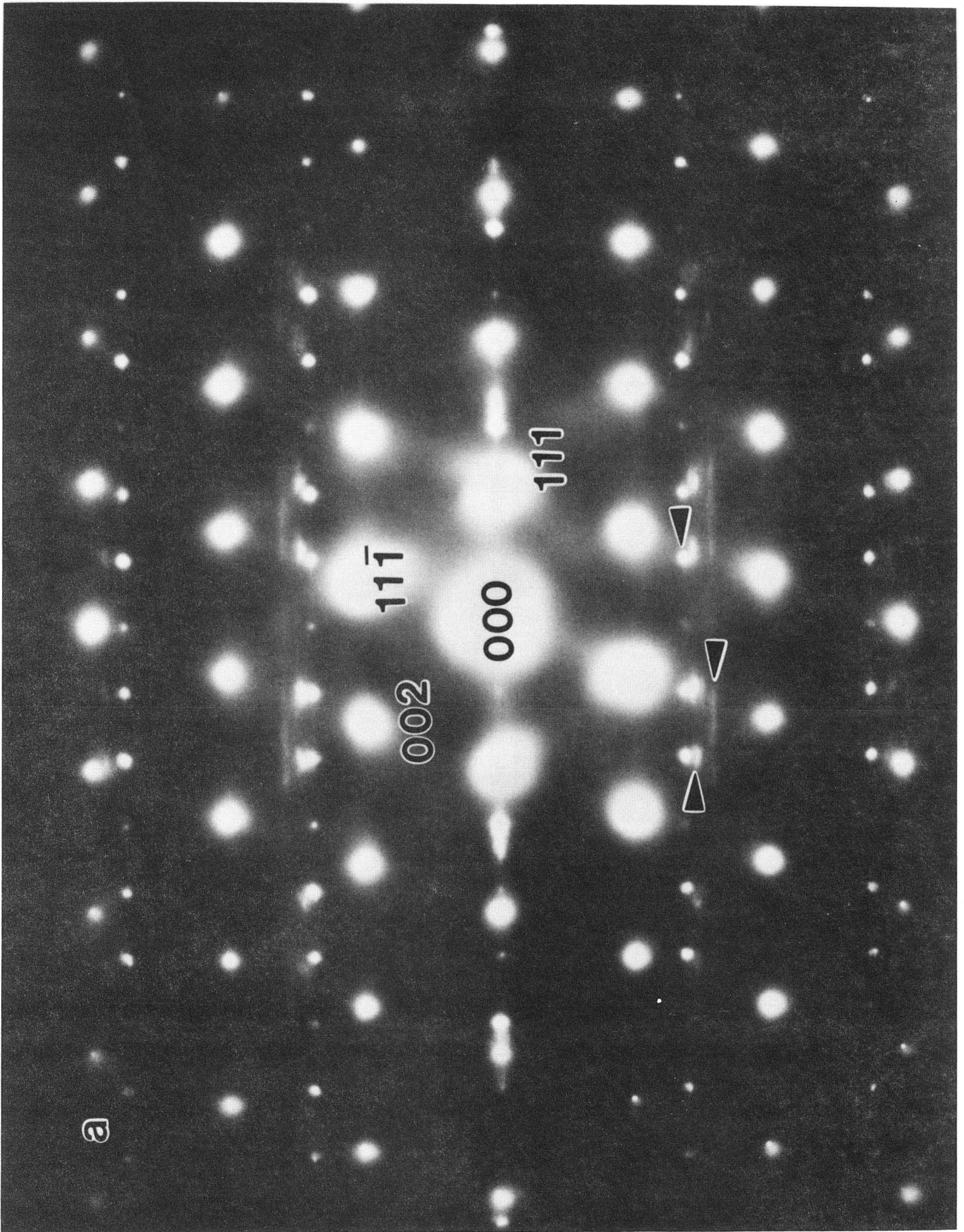
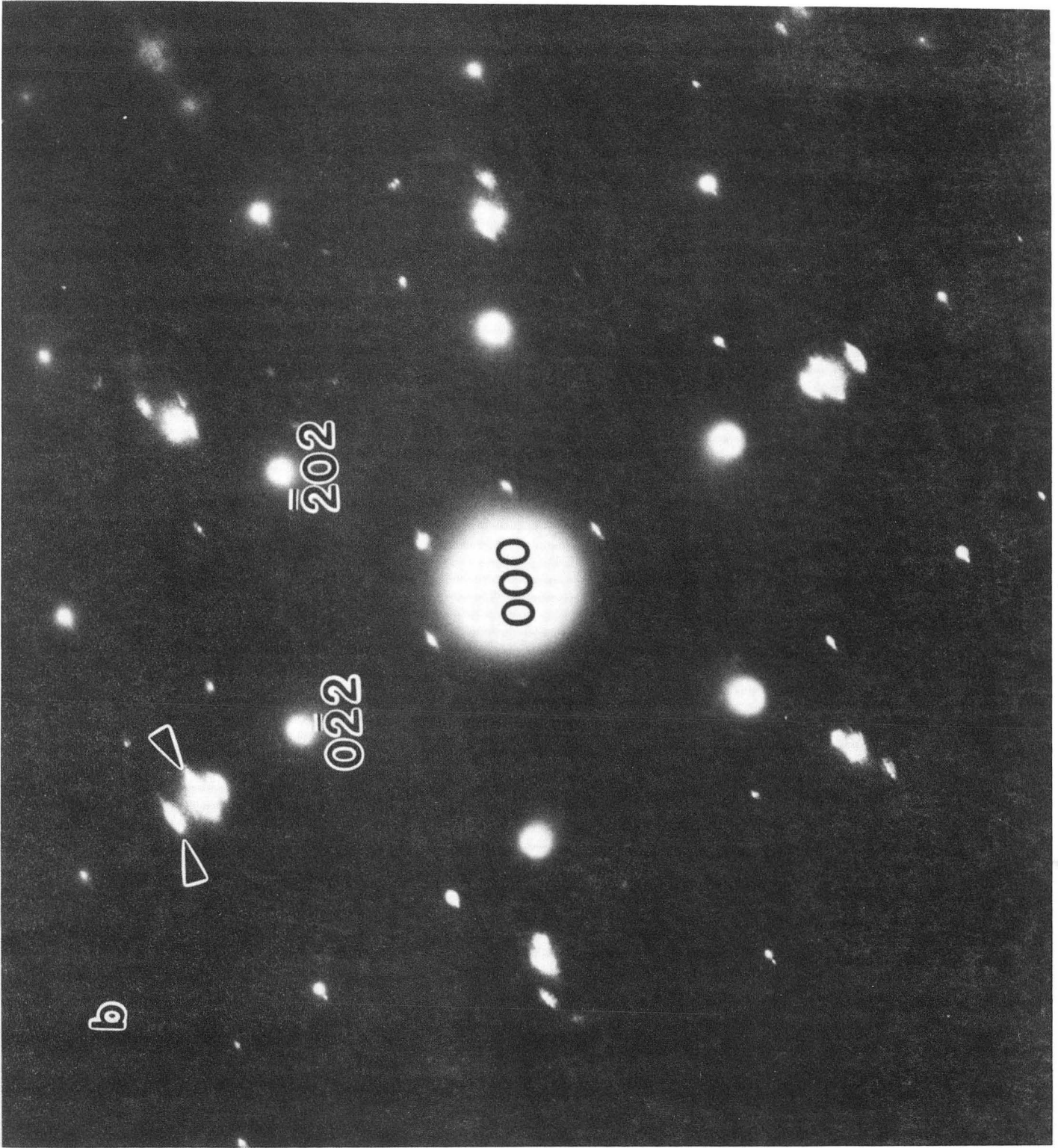


Figure 3c



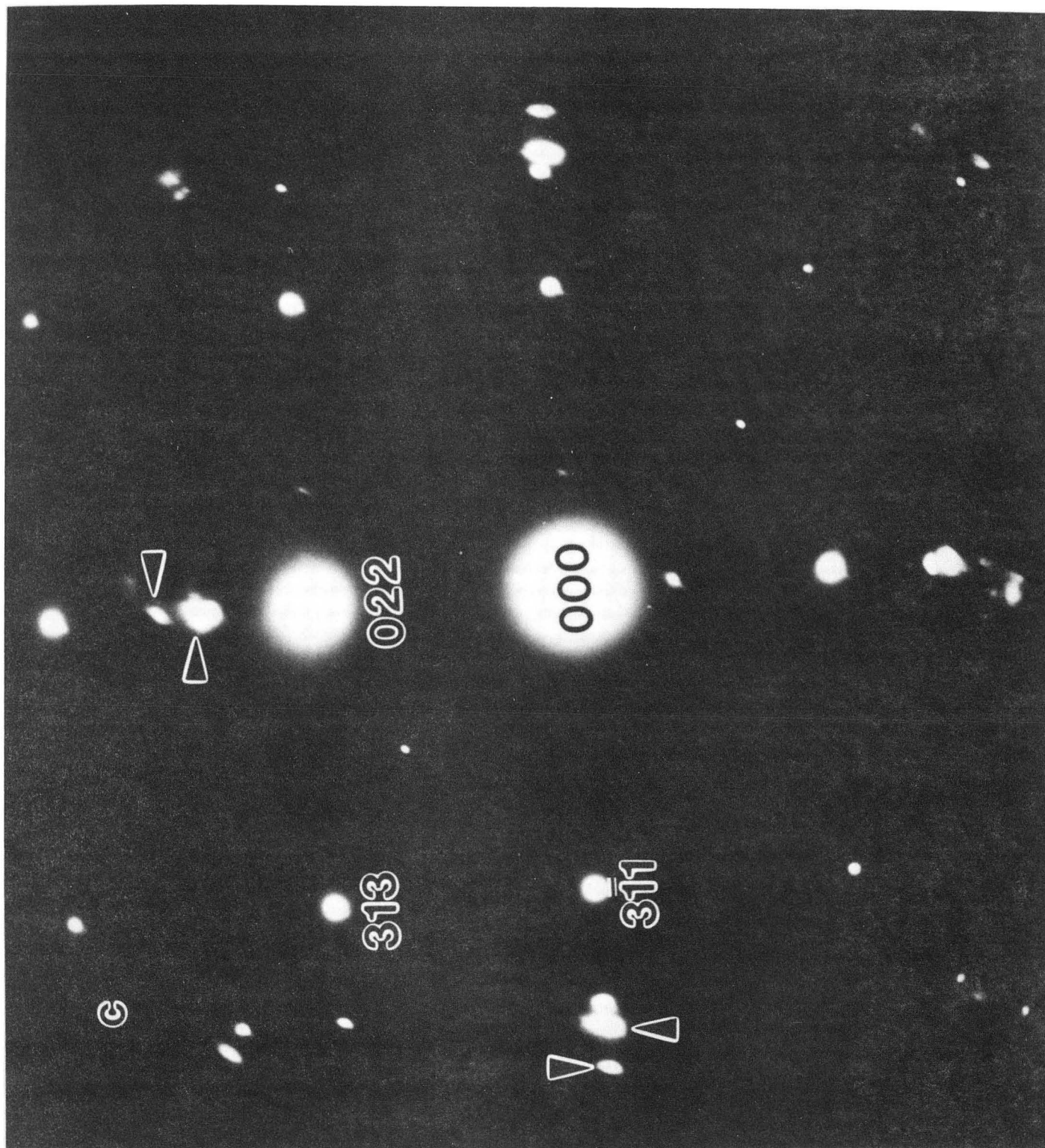
a

Figure 4a



XBB 925-3838

Figure 4b



XBB 925-3839

Figure 4c

LAWRENCE BERKELEY LABORATORY
UNIVERSITY OF CALIFORNIA
TECHNICAL INFORMATION DEPARTMENT
BERKELEY, CALIFORNIA 94720